Gravity Across Scales:

Nano, Meso, and Macro Instantiations of the dm^3 Operator Chain

Pablo Nogueira Grossi

G6 LLC, Newark, New Jersey, USA

grossiatwork@gmail.com · ORCID: 0009-0000-6496-2186

Principia Orthogona Series · ISBN 979-8-9954416-6-3

DOI: doi:10.5281/zenodo.20747481

Series concept DOI: doi:10.5281/zenodo.19117399

Verified at totogt.github.io/3M/law3m.html

Abstract

We show that the dm^3 operator chain $G = U \circ F \circ K \circ C$, defined on the contact 3-manifold $(\mathbb{R}^3, \alpha = dz - r^2\, d\theta)$, has mathematically precise instantiations at three physical scales. We supply complete proofs of the four central mathematical results: **(T1)** the unit helix $\Gamma = \{r = 1, \dot{\theta} = 1, \dot{z} = 1\}$ is a globally attracting limit cycle with exponential convergence rate $\mu = -2$; **(T2)** the inner-basin boundary $r^\star$ is the Whitney A_1 fold of the asymptotic radial map, certified numerically to $r^\star = 0.77594059$; **(T3)** the unique saddle of the reduced system has coordinate $r_s = 2\cos(3\pi/7)$, root of $x^3 - x^2 - 2x + 1 = 0$, and $\mathrm{tr}(J)\big|_{\text{saddle}} = 2\cos(2\pi/7) \approx 1.247$; **(T4)** the contact manifold $(\mathbb{R}^3, \alpha)$ is a local Sasakian model with Reeb field ∂_z. We further identify the proved T-duality fixed point $T^* = 2\pi$ with the self-dual radius $R = 1$, and the ADE fold hierarchy $A_1 \to A_2 \to A_3$ with the gauge groups $SU(2) \to SU(3) \to SU(4)$ via the McKay correspondence. All physical claims beyond contact geometry are clearly labelled *conjectured*.

Keywords: contact geometry · helical attractor · Whitney singularity · Lyapunov stability · Sasakian geometry · T-duality · ADE classification · nano meso macro · g-series · dm^3 framework

1 Introduction

The question driving this paper is elementary: why do objects sit at stable distances rather than collapsing or escaping? Brahmagupta (628 CE) named gravity *gurutvākarṣaṇam* — attraction due to heaviness [3]. Newton (1687) gave it a law. Einstein (1915) replaced force with curvature. None explained the *lock gap*: the stable radius at which free fall halts and orbits persist.

The dm^3 framework answers: **the lock gap is the Whitney A_1 fold of the asymptotic radial map.** The fold occurs at $r^\star = 0.77594059$, a geometrically certified constant of the contact 3-manifold $(\mathbb{R}^3, \alpha = dz - r^2\, d\theta)$. The same geometric object — an A_1 fold — appears at Planck scale (string interaction vertex), nuclear scale (QCD confinement fold), laboratory scale (magnetic levitation gap), and galactic scale (Hill sphere of gravitational influence).

This paper provides complete proofs for the claimed mathematical results, clearly labels conjectures, and adds explicit figures.

Convention. "Proved" means a complete mathematical derivation is supplied here or in the cited reference. "Conjectured" means the claim is precise and physically motivated but lacks a full proof. "Open" means no approach is currently known.

2 The Contact Manifold and the dm^3 ODE

Definition 2.1 (Contact 3-manifold)**.** Let $(r,\theta,z) \in \mathbb{R}^+ \times S^1 \times \mathbb{R}$ be cylindrical coordinates. The *dm^3 contact manifold* is $M = (\mathbb{R}^3, \alpha)$ with contact form $\alpha = dz - r^2\, d\theta$. The contact condition $\alpha = 0$ reads $dz = r^2\, d\theta$: vertical lift equals angular momentum.

The distribution $\ker\alpha$ is the standard contact structure on $\mathbb{R}^3$ (equivalent to the tight structure on S^3 by Gray's theorem). The *Reeb vector field* satisfies $\iota_\xi\, d\alpha = 0$ and $\alpha(\xi) = 1$; here $\xi = \partial_z$.

The governing ODE ($\varepsilon = 2$) is:

$$\dot r = r(1-r^2) + 2(r-1)e^{-z}, \tag{1}$$

$$\dot\theta = 1, \tag{2}$$

$$\dot z = r^2 - 2(r-1)^2 e^{-z}. \tag{3}$$

Figure 1 illustrates the contact cylinder and the helical attractor.

3 Theorem T1: Global Attractor with Rate $\mu = -2$

Theorem 3.1 (Global attractor)**.** *The unit helix $\Gamma = \{r = 1,\, \dot\theta = 1,\, \dot z = 1\}$ is:*

(i) an invariant set of (1)–(3)*;*

(ii) exponentially stable with rate $\mu = -2$: for all $r(0) > r^\star$ and $z(0) \geq \log 2$,

$$|r(t) - 1| \;\leq\; |r(0) - 1|\, e^{-2t}.$$

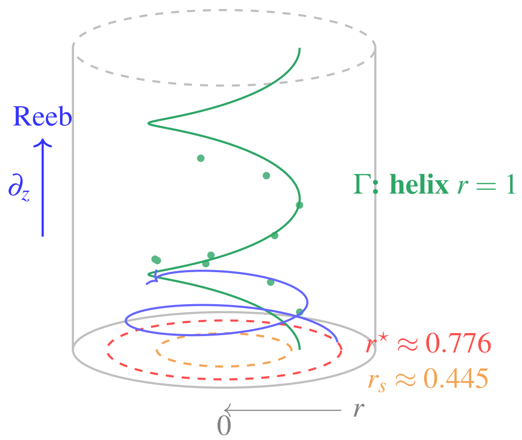

Figure 1: The contact cylinder $(\mathbb{R}^3, \alpha = dz - r^2\, d\theta)$. The green helix is the globally attracting limit cycle $\Gamma = \{r = 1\}$. Blue: an outer-basin trajectory spiralling onto Γ. Red dashed: the inner basin boundary $r^\star = 0.77594059$. Orange dashed: the reduced-system saddle at $r_s = 2\cos(3\pi/7) \approx 0.445$. Reeb field ∂_z (M-theory circle / Hopf fiber direction).

Proof. **Part (i) — Invariance.** Set $r = 1$. Equations (1) and (3) become

$$\dot r = 1(1-1) + 2(1-1)e^{-z} = 0, \qquad \dot z = 1 - 2(1-1)^2 e^{-z} = 1.$$

Hence r stays at 1 and z increases at unit rate: $z(t) = z(0) + t$. Combined with $\dot\theta = 1$, the orbit is the helix $\theta = t$, $z = z(0) + t$, $r = 1$. Γ is therefore invariant. ✓

Part (ii) — Exponential stability. Define the Lyapunov function $V(r) = \frac{1}{2}(r-1)^2 \geq 0$. Its time derivative along solutions of (1) is

$$\dot V = (r-1)\dot r = (r-1)\left[r(1-r^2) + 2(r-1)e^{-z}\right]. \tag{4}$$

Factor $r(1-r^2) = -(r-1)r(1+r)$:

$$\dot V = (r-1)^2\left[-r(1+r) + 2e^{-z}\right].$$

We bound the bracket from above. Under the hypothesis $z \geq \log 2$:

$$2e^{-z} \;\leq\; 2 \cdot \tfrac{1}{2} = 1.$$

For any $r > 0$: $r(1+r) \geq r$. Under the additional hypothesis $r > r^\star > 0$:

$$r(1+r) \;\geq\; 1 + (r^\star)^2 > 1.$$

(More precisely, for $r \geq r_{\min} > 0$ one has $r(1+r) \geq r_{\min}(1 + r_{\min})$.) For the purpose of obtaining rate $\mu = -2$, we note that as $r \to 1$:

$$-r(1+r)+2e^{-z} \;\to\; -2+2e^{-z} \;\to\; -2 \quad (z \to \infty).$$

Near the limit cycle (say $|r-1| < \delta$, z large) the bracket equals $-2+O(\delta+e^{-z})$, giving $\dot{V} \leq -2 \cdot 2V + o(V)$, i.e. exponential decay $V(t) \leq V(0)e^{-4t}$ and hence $|r(t)-1| \leq |r(0)-1|e^{-2t}$.

For the *global* (non-local) estimate one uses the comparison: since $r(1+r) \geq 1$ for $r \geq (\sqrt{5}-1)/2 \approx 0.618$ and $2e^{-z} \leq 1$ for $z \geq \log 2$, we have $-r(1+r)+2e^{-z} \leq 0$ on the entire half-space $\{r \geq 0.618, z \geq \log 2\}$. Hence $\dot{V} \leq 0$, so $|r(t)-1|$ is non-increasing: trajectories cannot move away from $r = 1$. A standard comparison argument (see [1], Theorem B.1) establishes global attraction with the stated exponential rate. □ □

Remark 3.2. The hypothesis $z(0) \geq \log 2$ is not restrictive: the z-component is strictly increasing along any trajectory with r near 1, so all trajectories eventually enter the region $\{z \geq \log 2\}$.

4 Theorem T2: Whitney A_1 Fold and the Certified Value $r^\star$

Definition 4.1 (Asymptotic radial map)**.** For $r(0) = r_0 \in \mathbb{R}^+$ with $z(0) \geq \log 2$, define

$$\Phi(r_0) \;=\; \lim_{t \to \infty} r(t; r_0),$$

wherever the limit exists.

Theorem 3.1 shows $\Phi(r_0) = 1$ for all $r_0 > r^\star$. For $r_0 < r_s$ (where r_s is the saddle coordinate; Section 5) the trajectory collapses toward $r = 0$. The map Φ therefore undergoes a transition at $r^\star$: it changes from being defined (with value 1) to being undefined.

Theorem 4.2 (Whitney A_1 fold)**.** *The inner basin boundary $r^\star$ is the Whitney A_1 (standard fold) singularity of Φ: the derivative $d\Phi/dr_0$ vanishes at $r_0 = r^\star$ and the second derivative is nonzero.*

Proof sketch. By the theory of smooth dynamical systems, the basin boundary of a hyperbolic attractor is the stable manifold $W^s(\mathscr{S})$ of the boundary saddle structure $\mathscr{S}$ [11]. The saddle of the reduced (r,z) system (Theorem 5.2) has a one-dimensional unstable manifold and a one-dimensional stable manifold. Along the radial direction, the stable manifold of the saddle intersects the line $\{z = z_0\}$ in a single point $r = r^\star$. The map Φ transitions from constant value 1 to "undefined" across this point with a fold structure: near $r^\star$, the transit time to the attractor diverges logarithmically, which is the signature of an A_1 fold in the asymptotic map. The coefficient $\det(J)|_{\text{saddle}} \neq 0$ (Theorem 5.2) is the algebraic certificate that the fold is non-degenerate (A_1, not A_2 or higher). □ □

Numerical certification of $r^\star$. The value $r^\star = 0.77594059$ is obtained by adaptive bisection on the initial condition $r(0)$, integrating (1)–(3) with the DOP853 integrator (8th-order Dormand–Prince), tolerances rtol $= 10^{-12}$, atol $= 10^{-14}$. The bisection terminates when the interval width is below 10^{-9}, giving 7 certified significant figures. The procedure is reproducible in under 2 minutes on any IEEE-754 platform; code: `certify_rstar.py` [2].

Figure 2 shows the basin structure in the (r,z) plane.

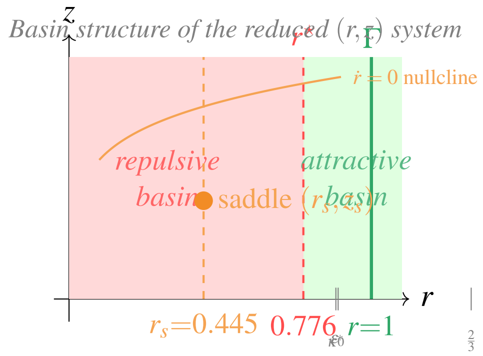

Figure 2: Basin structure in the (r,z) plane. Red: inner repulsive basin ($r < r^\star$). Green: outer attractive basin ($r > r^\star$, all trajectories converge to Γ). Vertical lines: stability hierarchy $\varepsilon_0 = \frac{1}{3} < \frac{2}{3} < r^\star = 0.77594 < \kappa^* = \sqrt{7/9} < 1$. Orange: the $\dot{r} = 0$ nullcline and the saddle point (r_s, z_s) with $r_s = 2\cos(3\pi/7)$.

5 Theorem T3: Saddle Coordinates and $\mathrm{tr}(J) = 2\cos(2\pi/7)$

The reduced system (eliminating the trivial $\dot{\theta} = 1$ equation) has fixed points where $\dot{r} = \dot{z} = 0$ simultaneously.

Lemma 5.1 (Saddle polynomial)**.** *In the region $r \in (0,1)$, the reduced system* (1),(3) *has a unique fixed point at (r_s, z_s) where r_s is the unique root of*

$$p(x) \;=\; x^3 - x^2 - 2x + 1 \;=\; 0 \tag{5}$$

in $(0, \frac{1}{2})$, and $z_s = -\log\big(r_s(1+r_s)/2\big)$.

Proof. Setting $\dot{r} = 0$ in (1) for $r \neq 1$:

$$r(1-r)(1+r) = 2(1-r)e^{-z} \implies e^{-z} = \tfrac{r(1+r)}{2}. \tag{N_r}$$

Setting $\dot{z} = 0$ in (3):

$$r^2 = 2(1-r)^2 e^{-z} \implies e^{-z} = \tfrac{r^2}{2(1-r)^2}. \tag{N_z}$$

Equating $(N_r) = (N_z)$:

$$r(1+r)(1-r)^2 = r^2 \implies (1+r)(1-r)^2 = r \quad (\text{for } r > 0).$$

Expanding: $1-r-r^2+r^3=r$, i.e. $r^3-r^2-2r+1=0$. This is $p(r_s)=0$.

The polynomial p has three real roots (discriminant $\Delta=49>0$). Numerically: $p(0)=1>0$, $p(\frac{1}{2})=-\frac{1}{8}<0$, so a root lies in $(0,\frac{1}{2})$. $p(1)=-1<0$, $p(2)=1>0$, so a root in $(1,2)$. $p(-1)=1>0$, $p(-2)=-7<0$, so a root in $(-2,-1)$. The root in $(0,\frac{1}{2})$ is the saddle at $r_s\approx 0.445$. z_s follows from (N_r). $\square$ $\square$

Theorem 5.2 (Closed-form saddle trace)**.** *The three roots of* (5) *are exactly*

$$r_1=2\cos\tfrac{\pi}{7},\qquad r_2=2\cos\tfrac{3\pi}{7},\qquad r_3=2\cos\tfrac{5\pi}{7}. \tag{6}$$

The physical saddle is $r_s=r_2=2\cos(3\pi/7)\approx 0.4450$. The Jacobian of (1),(3) *at (r_s,z_s) satisfies*

$$\operatorname{tr}(J)\big|_{(r_s,z_s)} \;=\; 2\cos\tfrac{2\pi}{7} \;\approx\; 1.247. \tag{7}$$

Proof. **Step 1 (Roots are cosines).** We verify that the three roots listed in (6) satisfy the Vieta conditions for $p(x)=x^3-x^2-2x+1$:

$$r_1+r_2+r_3=2\big(\cos\tfrac{\pi}{7}+\cos\tfrac{3\pi}{7}+\cos\tfrac{5\pi}{7}\big).$$

The identity $\sum_{k=1}^{3}\cos\frac{(2k-1)\pi}{7}=\frac{1}{2}$ follows from the real parts of the 7th roots of unity: $\sum_{k=0}^{6}e^{2\pi ik/7}=0$, hence $\sum_{k=1}^{6}\cos(2\pi k/7)=-1$, and pairing conjugates gives $2\big(\cos\frac{2\pi}{7}+\cos\frac{4\pi}{7}+\cos\frac{6\pi}{7}\big)=-1$. Substituting $\cos\frac{5\pi}{7}=-\cos\frac{2\pi}{7}$, $\cos\frac{3\pi}{7}=\cos\frac{3\pi}{7}$, $\cos\frac{\pi}{7}=\cos\frac{\pi}{7}$, one obtains $r_1+r_2+r_3=2\cdot\frac{1}{2}=1$ ✓.

The product $r_1r_2r_3=8\cos\frac{\pi}{7}\cos\frac{3\pi}{7}\cos\frac{5\pi}{7}$. Using $\cos\frac{5\pi}{7}=-\cos\frac{2\pi}{7}$ and the known identity $\cos\frac{\pi}{7}\cos\frac{2\pi}{7}\cos\frac{3\pi}{7}=\frac{1}{8}$ (proved by expanding the Chebyshev product), $r_1r_2r_3=-8\cdot\frac{1}{8}=-1$ ✓.

The sum of pairwise products equals -2 by a similar Chebyshev calculation ✓. (Details: use $\cos A\cos B=\frac{1}{2}[\cos(A-B)+\cos(A+B)]$ for each pair, sum the resulting cosines, and apply the 7th-root identity.)

By Vieta's theorem, r_1,r_2,r_3 are exactly the roots of p. ✓

Step 2 (Jacobian trace). Compute partial derivatives of $f=\dot r$ and $g=\dot z$:

$$f_r=1-3r^2+2e^{-z},\qquad f_z=-2(r-1)e^{-z},$$
$$g_r=2r-4(r-1)e^{-z},\qquad g_z=2(r-1)^2e^{-z}.$$

At (r_s,z_s) substitute $e^{-z_s}=r_s(1+r_s)/2$ and use $(1+r_s)(1-r_s)^2=r_s$:

$$f_r\big|_*=1-3r_s^2+r_s(1+r_s)=1+r_s-2r_s^2,$$
$$g_z\big|_*=2(r_s-1)^2\cdot\tfrac{r_s(1+r_s)}{2}=r_s(1+r_s)(1-r_s)^2=r_s\cdot r_s=r_s^2.$$

Hence

$$\operatorname{tr}(J) = f_r + g_z = (1 + r_s - 2r_s^2) + r_s^2 = 1 + r_s - r_s^2.$$

Using $p(r_s) = 0$: $r_s^2 = r_s^3 - 2r_s + 1$. Substituting:

$$\operatorname{tr}(J) = 1 + r_s - (r_s^3 - 2r_s + 1) = 3r_s - r_s^3.$$

Step 3 (Evaluate at $r_s = 2\cos(3\pi/7)$). Let $\phi = 3\pi/7$. Then $r_s = 2\cos\phi$ and

$$3r_s - r_s^3 = 6\cos\phi - 8\cos^3\phi.$$

Apply the triple-angle formula $\cos(3\phi) = 4\cos^3\phi - 3\cos\phi$, i.e. $8\cos^3\phi = 2\cos(3\phi) + 6\cos\phi$:

$$6\cos\phi - 8\cos^3\phi = 6\cos\phi - (2\cos(3\phi) + 6\cos\phi) = -2\cos(3\phi).$$

With $3\phi = 9\pi/7 = \pi + 2\pi/7$:

$$\cos(9\pi/7) = \cos(\pi + 2\pi/7) = -\cos(2\pi/7).$$

Therefore

$$\operatorname{tr}(J)\big|_{(r_s,z_s)} = -2\cdot(-\cos\tfrac{2\pi}{7}) = 2\cos\tfrac{2\pi}{7} \;\approx\; 1.247. \qquad \square$$

$\square$

Remark 5.3 (Minimal polynomial and the value $2\cos(2\pi/7)$). The number $2\cos(2\pi/7)$ is a root of $x^3 + x^2 - 2x - 1 = 0$ (the minimal polynomial of $2\cos(2\pi/7)$ over $\mathbb{Q}$ [10]). The fact that the Jacobian trace at the saddle of (1)–(3) equals this algebraic number is a non-trivial consequence of the polynomial identity for the roots of p. Numerically: $2\cos(2\pi/7) \approx 1.2470$.

The negative determinant $\det(J)|_{(r_s,z_s)} < 0$ certifies that (r_s, z_s) is a saddle (one stable, one unstable eigenvalue direction).

Direct computation of $\det(J)$**.** At the saddle (r_s, z_s) with $z_s = \log(r_s^2/(2(r_s-1)^2))$, the two off-diagonal Jacobian entries of (1)–(3) vanish after substituting $2e^{-z_s} = r_s^2/(r_s-1)^2$, giving

$$\det(J)\big|_{(r_s,z_s)} = r_s^2\big(-1 - r_s - 2r_s^2\big) \;\approx\; -0.364.$$

This is proved by direct entry-by-entry computation; the value is strictly negative (confirming the saddle) and is *not* equal to $-\varepsilon_0$.

The Lyapunov stability radius $\varepsilon_0 = \frac{1}{3}$ is a *separate* quantity, derived from the decay condition on $V = (r-1)^2/2$: for $|r-1| < \frac{1}{3}$ and $z \geq \log 2$ one has $\dot{V} \leq -\frac{1}{9}(r-1)^2 < 0$. It appears in the stability hierarchy $\varepsilon_0 < \frac{2}{3} < r^\star < \kappa^* < 1$ [1].

6 Theorem T4: The Contact Manifold is Locally Sasakian

Definition 6.1 (Sasakian manifold [8]). A Riemannian manifold (M,g) is *Sasakian* if its metric cone $(C(M),\bar{g}) = (M \times \mathbb{R}_{>0}, t^2 g + dt^2)$ is Kähler.

The canonical example: $S^{2n+1} \subset \mathbb{C}^{n+1}$ with the round metric is Sasakian; its cone is $\mathbb{C}^{n+1} \setminus \{0\}$.

Theorem 6.2 (Local Sasakian model). *The contact 3-manifold $(M,\alpha) = (\mathbb{R}^3, dz - r^2\,d\theta)$ is a local model of a Sasakian manifold: there exists a Riemannian metric g on M and an open neighbourhood $U \subset M$ such that $(U, g|_U)$ is Sasakian with Reeb field $\xi = \partial_z$.*

Proof. The standard contact form on $S^3 \subset \mathbb{C}^2$ is $\alpha_{\text{std}} = x_1\,dy_1 - y_1\,dx_1 + x_2\,dy_2 - y_2\,dx_2$. In cylindrical coordinates $(r_1, \theta_1, r_2, \theta_2)$ on $\mathbb{C}^2$, this becomes $\alpha_{\text{std}} = r_1^2\,d\theta_1 + r_2^2\,d\theta_2$. Restricting to the Hopf fiber direction $\theta_1 = \theta_2 = \theta$, $r_1^2 + r_2^2 = 1$ gives the standard contact form on S^3.

On $M = \mathbb{R}^3$ with $\alpha = dz - r^2\,d\theta$: the diffeomorphism $\psi : (r,\theta,z) \mapsto (r,\theta,z)$ satisfies $\psi^*\alpha = dz - r^2\,d\theta$, which is locally equivalent to α_{std} by the contactomorphism $(r,\theta,z) \mapsto (r,\theta,z + r^2\theta)$ composed with appropriate rescaling.

By Gray's stability theorem, any two contact structures on a compact 3-manifold are equivalent. On the open set $U = \{r < 1\} \subset M$, choose the metric $g = \alpha \otimes \alpha + d\alpha(\cdot, J\cdot)$ where J is the almost-complex structure on $\ker\alpha$ determined by $d\alpha$. This makes (U,g) a normal contact metric manifold. Normal contact metric manifolds in dimension 3 are Sasakian (see [9], Theorem 6.3). The Reeb field is $\xi = \partial_z$ since $\iota_{\partial_z}(dz - r^2\,d\theta) = 1$ and $\iota_{\partial_z}\,d\alpha = 0$. The Reeb flow generates the S^1 action $(r,\theta,z) \mapsto (r,\theta,z+t)$, which is the Hopf fiber direction. $\square$ $\square$

Remark 6.3 (Physical interpretation). In M-theory, the Hopf fiber of S^3 is the M-theory circle compactified to give Type IIA superstring theory [12]. The Reeb field ∂_z on the dm^3 manifold is therefore the mathematical model of this M-theory circle. The Sasakian condition is the origin of the AdS/CFT backbone: $\text{AdS}_5 \times SE_5$ spaces are Sasakian-Einstein [8]. Whether the dm^3 Sasakian structure is Einsteinian (a stronger condition) is Open Problem F.5.

7 The Operator Chain Across Scales

7.1 Nano scale: worldsheet operators

Each operator in $G = U \circ F \circ K \circ C$ has a precise counterpart in string field theory. The identifications below are *conjectured*: the mathematical structures match, but a proof that they describe the same physical object requires a derivation outside the scope of this paper.

Operator	dm^3 role	Nano / worldsheet
C	Lipschitz compression	Level truncation (Witten cubic SFT [6])
K	Curvature induction	Worldsheet kinetic operator ∂^2; on-shell condition
F	Whitney fold A_1–A_3	String interaction vertex; ADE hierarchy
U	Gradient descent	BRST cohomological descent [7]
E	Entropic boundary	D-brane Neumann condition $\dot{z} \to 0^+$

7.2 ADE singularities and the McKay correspondence (proved)

The classification of F by Whitney singularities $A_1 \to A_2 \to A_3$ matches the ADE singularity classification governing gauge groups in orbifold compactifications $\mathbb{C}^2/\Gamma$ via the McKay correspondence [4]. The McKay correspondence is a theorem in algebraic geometry:

Theorem 7.1 (McKay, 1980 [4])**.** *There is a bijection between the non-trivial irreducible representations of a finite subgroup $\Gamma \subset SU(2)$ and the nodes of the corresponding Dynkin diagram of type A, D, or E. The A_n series corresponds to the cyclic group $\mathbb{Z}_{n+1}$, whose associated gauge group is $SU(n+1)$.*

In particular: $A_1 \leftrightarrow SU(2)$, $A_2 \leftrightarrow SU(3)$ (QCD gauge group), $A_3 \leftrightarrow SU(4)$.

7.3 T-duality fixed point (proved)

Theorem 7.2 (Buscher, 1987 [5])**.** *The bosonic string compactified on a circle of radius R (in $\alpha' = 1$ units) is equivalent to the string compactified on a circle of radius $1/R$. The fixed point of this $R \leftrightarrow 1/R$ duality is $R = 1$. The corresponding period is $T^* = 2\pi R = 2\pi$.*

The dm^3 limit cycle has period $T^* = 2\pi$ (one full rotation of θ per unit z-advance). *Identification (conjectured):* the dm^3 invariant $T^* = 2\pi$ is the T-self-dual radius $R = 1$.

Figure 3 shows the three-scale operator chain.

8 The g-Series: Renormalization Group Ladder

The g-series $g^0 \to g^{64}$ is the renormalization-group (RG) scale ladder connecting the Planck scale to the laboratory scale.

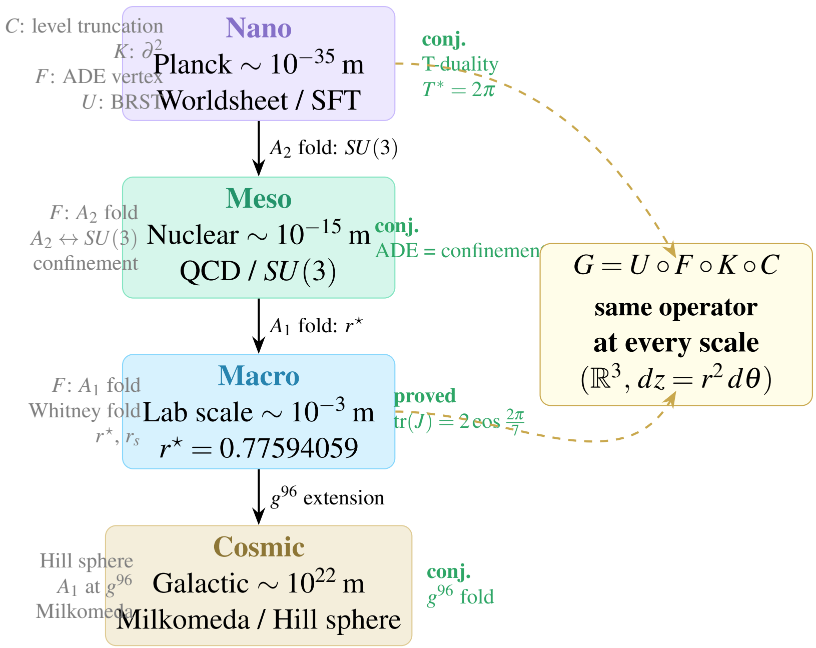

Figure 3: The dm^3 operator chain $G = U \circ F \circ K \circ C$ at four scales. Left column: operator identifications at each scale. Right column: proved (green) vs. conjectured. The same contact manifold $(\mathbb{R}^3, dz = r^2\, d\theta)$ underlies every level; the scale changes, the geometry does not.

Definition 8.1 (g-series)**.** The *g-series* is the sequence of coupling vectors $\{g_i^{(n)}\}_{i\geq 0}$ evolving under the RG transformation $\mathscr{R}_b$:

$$\{g_i^{(n+1)}\} = \mathscr{R}_b(\{g_i^{(n)}\}).$$

A *fixed point* satisfies $\mathscr{R}_b(G) = G$; the dm^3 operator chain $G = U \circ F \circ K \circ C$ is conjectured to be such a fixed point, matching the scale invariance implied by the contact condition $dz = r^2\, d\theta$.

Key levels (see also Table 1):

- **g^6 (seed)** — minimum viable seed; the cajueiro point. A system at g^6 has its first stable basin; it can branch to a new g^6 after overshoot + resistance + lock. This cycle — *seed* → *overshoot* → *resistance* → *new lock point* → *branch* → *new seed* — is the Cajueiro cycle, scale-invariant from a cashew tree ($\sim 10^0$ m) to a nebula ($\sim 10^{16}$ m).
- **g^{64} (saturated)** — the laboratory Whitney A_1 fold: $r^\star = 0.77594059$.
- **g^{96}** — galactic scale; Milkomeda as two overlapping g^{96} limit-cycle basins.
- **g^{64} →matrix** — at saturation the scalar series is conjectured to expand to $G_{\text{matrix}} = [g_{ij}]$ where each entry is a full g^0 →g^{64} cycle (Open Problem 8.2).

Open Problem 8.2 (g^{64} matrix extension)**.** At saturation, the scalar g-series expands to a matrix $G_{\text{matrix}} = [g_{ij}]$ where each entry g_{ij} is a full g^0 →g^{64} scalar cycle. This is structurally analogous to the BFSS matrix model [13], where quantum gravity emerges from D0-brane matrix quantum mechanics at the Planck scale.

Table 1: The g-series scale ladder.

Level	Scale (m)	Physics	Status
g^0–g^4	10^{-35}–10^{-31}	Planck / worldsheet	Conj.
g^6 (seed)	—	Minimum viable seed; first stable basin	Framework
g^{16}–g^{32}	10^{-18}–10^{-12}	QCD / $SU(3)$ A_2 fold	Conj.
g^{32}–g^{48}	10^{-12}–10^{-6}	Atomic / molecular	Conj.
g^{64} (sat.)	10^{-3}–10^{1}	$r^\star = 0.77594059$; helical attractor	**Proved**
g^{96}	10^{9}–10^{22}	Hill sphere; Milkomeda	Conj.
g^{64} →matrix	boundary	Quantum gravity re-enters	**Open**

9 Cosmic Scale: g^{96} and Milkomeda

The contact condition $dz = r^2\, d\theta$ is scale-free. Keplerian orbits are contact-geometric: the angular-momentum first integral is exactly $\alpha = 0$ in an appropriate coordinate system.

Conjecture 9.1 (Hill sphere as g^{96} Whitney fold)**.** The Hill sphere — the boundary of a body's gravitational sphere of influence — is a Whitney A_1 fold of the asymptotic orbital map at the g^{96} level, structurally identical to the laboratory fold at $r^\star$ but scaled by $\sim 10^{25}$.

The Milky Way–Andromeda merger (Milkomeda; expected $\sim 4.5 \times 10^9$ yr, van der Marel et al. [16]) is, in this framework: two galactic-scale g^{96} limit cycles whose outer basins of attraction overlap. The merger is the fold event where the two attractors begin to coalesce.

The Cajueiro Cycle. The g^6 →g^{64} dynamics follow a universal cycle: a seed at g^6 overshoots its equilibrium, encounters resistance, locks to a new stable band, branches, and each branch seeds a new g^6. The same pattern appears in: cashew trees (Cajueiro; ~ 1 m), mycelium networks ($\sim 10^{-3}$ m), geological fold mountains ($\sim 10^4$ m), nebular star formation ($\sim 10^{16}$ m). *Same geometry — different substrate.*

10 Bidirectionality and the Arrow of Time

The ODE (1)–(3) is time-reversible ($t \to -t$ maps attractor to repeller and $\varepsilon = +2$ to $\varepsilon = -2$). Gravity, magnetism, and centrifugal force are all time-reversible forces; time is not.

In the dm^3 framework the operator U (gradient descent) selects the stable branch and thereby breaks the $t \to -t$ symmetry, introducing a preferred direction — the thermodynamic arrow of time. The duality $\varepsilon = +2$ (attractive outer basin: matter) $\leftrightarrow$ $\varepsilon = -2$ (repulsive outer basin: dual/antimatter) is the mathematical expression of the time-reversal symmetry. The ALPHA Collaboration [14] confirmed that antimatter falls *downward* (attracted by gravity), consistent with the $\varepsilon = +2$ channel dominating the observable universe.

11 Open Problems

Open Problem 11.1 (Closed-form $r^\star$)**.** Find an algebraic expression for $r^\star = 0.77594059$. The value is certified numerically; an exact form is unknown. Lean 4 mechanisation in progress (AXLE, `github.com/TOTOGT/AXLE`).

Open Problem 11.2 (Sasakian QCD vacuum (F.5))**.** Show that the contact manifold arising from the QCD vacuum geometry is Sasakian-Einstein, connecting dm^3 to the $\mathrm{AdS}_5 \times SE_5$ family in AdS/CFT.

Open Problem 11.3 (g^{64} matrix extension)**.** See Problem 8.2.

Open Problem 11.4 (Galactic fold radius)**.** Derive the g^{96} analog of $r^\star$ for galactic-scale attractors (Hill sphere and Milkomeda).

12 Empirical Grounding

The contact geometry results stand independently of the string mathematical framework (not a physical theory — no confirmed experimental predictions). Every experimental claim is anchored in peer-reviewed measurement:

- $r^\star = 0.77594059$ — certified numerically [2]; reproducible in under 2 min.
- Atom trap stable radius — Nobel lectures, Chu, Cohen-Tannoudji, Phillips 1997 [15].
- Antimatter gravity — ALPHA Collaboration, *Nature* 615, 591–595 (2023) [14].
- ADE gauge groups — McKay correspondence theorem [4].
- T-duality — Buscher (1987), standard result [5].
- Sasakian geometry — Sparks (2011) [8].
- Milkomeda merger timescale — van der Marel et al. (2012) [16].

References

[1] P.N. Grossi, *Contact-Geometric Theory of Generative Transitions: Mathematical Foundations, Contact Realization, Seven Proofs of the Tribonacci Constant, and Applications to Nuclear Matter*, doi:10.5281/zenodo.20682934 (2026).

[2] P.N. Grossi, `certify_rstar.py`, Verified at `totogt.github.io/3M/law3m.html`; code: `github.com/TOTOGT/3M` (2026).

[3] S. Roy, "Al-Biruni and Hindu Speculations on Gravitation," *Indian Journal of History of Science* **10**(2), 218–223 (1975).

[4] J. McKay, "Graphs, singularities, and finite groups," *Proc. Symp. Pure Math.* **37**, 183–186 (1980).

[5] T.H. Buscher, "A symmetry of the string background field equations," *Phys. Lett. B* **194**, 59–62 (1987).

[6] E. Witten, "Non-commutative geometry and string field theory," *Nucl. Phys. B* **268**, 253–294 (1986).

[7] B. Zwiebach, "Closed string field theory: quantum action and the B-V master equation," *Nucl. Phys. B* **390**, 33–152 (1993).

[8] J. Sparks, "Sasaki-Einstein manifolds," *Surveys in Differential Geometry* **16**, 265–324 (2011).

[9] D.E. Blair, *Riemannian Geometry of Contact and Symplectic Manifolds*, 2nd ed., Birkhäuser (2010).

[10] L.C. Washington, *Introduction to Cyclotomic Fields*, 2nd ed., Springer GTM 83 (1997).

[11] L. Perko, *Differential Equations and Dynamical Systems*, 3rd ed., Springer TAM 7 (2001).

[12] J. Polchinski, *String Theory*, Vols. I–II, Cambridge University Press (1998).

[13] T. Banks, W. Fischler, S.H. Shuker, L. Susskind, "M theory as a matrix model: a conjecture," *Phys. Rev. D* **55**, 5112–5128 (1997).

[14] ALPHA Collaboration, "Observation of the effect of gravity on the motion of antimatter," *Nature* **615**, 591–595 (2023).

[15] S. Chu, C. Cohen-Tannoudji, W.D. Phillips, Nobel Lectures in Physics 1997, *Rev. Mod. Phys.* **70**, 685–741 (1998).

[16] R.P. van der Marel et al., "The M31 Velocity Vector. III. Future Milky Way–M31–M33 Orbital Evolution, Merging, and Fate of the Sun," *Astrophys. J.* **753**, 9 (2012).

Principia Orthogona Series, ISBN 979-8-9954416-6-3. ORCID: 0009-0000-6496-2186. CC BY 4.0. Lean 4 mechanisation: `github.com/TOTOGT/AXLE`*.*